Improvement of Mechanical Properties of Spheroidized 1045 Steel by Induction Heat Treatment

MINWOOK KIM, JUNG-HO SHIN, YOUNG CHOI, and SEOK-JAE LEE

The effects of induction heat treatment on the formation of carbide particles and mechanical properties of spheroidized 1045 steel were investigated by means of microstructural analysis and tensile testing. The induction spheroidization accelerated the formation of spherical cementite particles and effectively softened the steel. The volume fraction of cementite was found to be a key factor that affected the mechanical properties of spheroidized steels. Further tests showed that sequential spheroidization by induction and furnace heat treatments enhanced elongation within a short spheroidization time, resulting in better mechanical properties. This was due to the higher volume fraction of spherical cementite particles that had less diffusion time for particle coarsening.

DOI: 10.1007/s11661-016-3327-8

I. INTRODUCTION

SPHEROIDIZATION is an important heat treatment process to increase the ductility of steels that undergo considerable deformation at room temperature.[1] During spheroidization, a steel specimen is typically held at a temperature below the A_{e1} temperature (*e.g.*, 973 K (700 °C)) for a long time (12 to 20 hours), which causes the formation of highly stable spheroidized cementite particles dispersed in a ferrite matrix. Pearlite with a lamellar structure composed of plate-type cementite particles and a ferrite matrix is transformed just below the A_{e1} temperature during the austenite decomposition. The cementite lamellae divide into small spherical cementite particles. The driving force for the spherical particle formation is the reduction in the surface energy caused by a decrease in the ratio of the interfacial surface area to the unit volume between ferrite and cementite. The total interfacial surface area can be minimized by growing or merging the small cementite particles during spheroidization, which is referred to as coarsening or Ostwald ripening.[2]

The spheroidization of steels is a prolonged heat treatment, typically lasting several tens of hours. Many researchers have investigated the potential reduction in the spheroidization process time over the last few decades. The use of cycling heat treatment is effective for accelerating the spheroidization process. Chou *et al.*[3] obtained a spheroidized structure of hypoeutectoid steel with 0.45 wt pct C brought about after quenching a sample to a lower temperature and immediately heating it to the spheroidization temperature below A_{c1}. During this thermal cycle, supercooled austenite was directly decomposed into spheroidized cementite that was homogeneously distributed in a ferrite matrix. Saha *et al.*[4,5] proposed the cyclic annealing of steel with 0.6 wt pct C to accelerate spheroidization. Their sample was repeatedly heated to a temperature higher than the A_{c3} temperature and immediately quenched to room temperature. This process produced almost fully spheroidized cementite after 8 cycles. Lv *et al.*[6] investigated the cementite spheroidization behavior in Fe-0.8 pctC steel during repeated cyclic heat treatment. They found that as the number of cyclic treatments was increased, the fraction of spheroidized cementite increased and that spheroidization was completed after five cyclic treatments.

Other studies have found that deformation can promote the kinetics of faster spheroidization. Nam and Lee[7] achieved the rapid spheroidization of high-carbon steel wire by drawing at temperatures between 873 K and 973 K (600 °C and 700 °C). They reported that the diffusion of carbon and iron dramatically increased as dislocations and vacancies were regenerated during drawing at high temperatures. Zhang *et al.*[8] designed processing routes using hot deformation to achieve the spheroidized microstructure in high-carbon steel. Their sample was deformed near the A_{e1} temperature and slowly cooled to room temperature. The deformation resulted in dislocations that contributed to the formation of spheroidized cementite. Guo *et al.*[9] investigated a subcritical spheroidization

MINWOOK KIM, Graduate Student, and SEOK-JAE LEE, Assistant Professor, are with the Division of Advanced Materials Engineering, Research Center for Advanced Materials Development, Chonbuk National University, Jeonju 561-756, Republic of Korea. Contact e-mail: seokjaelee@jbnu.ac.kr JUNG-HO SHIN, Principal Researcher, is with the Product Research Center, R&D Center, SeAH Besteel, Soryong-dong, Gunsan 573-711, Republic of Korea. YOUNG CHOI, Senior Researcher, is with the Convergence Components and Agricultural Machinery Application Group, Jeonbuk Regional Division, KITECH, 222 Palokro, Jeonju 561-202, Republic of Korea.

Manuscript submitted June 21, 2015.
Article published online January 19, 2016

annealing of cold-rolled 50CrV4 steel in which the formation of spheroidized cementite was accelerated by the cold rolling deformation. Furthermore, they found that the occurrence of spheroidization was promoted by applying more severe deformation. Arruabarrena *et al.*[10] applied warm deformation to promote spheroidization kinetics in 5140 steel. The warm deformation brought about the fragmentation of cementite lamellae and the formation of defects in the cementite and ferrite matrix, resulting in faster lamellae break-up and reduced spheroidization time.

Still other factors such as the alloying elements, initial microstructure, and thermal schedule have been investigated. O'Brien and Hosford[11] reported that in the case of the 4037 steel, subcritical annealing, rather than intercritical annealing, is necessary to achieve shorter spheroidization time. Li *et al.*[12] achieved very fine spheroidized cementite particles dispersed uniformly in a recrystallized ferrite matrix from the austenite with inhomogeneous carbon concentration in ultra-high-carbon steel containing 1.55 pct C and 1.5 pct Al. Karnyabi-Gol and Sheikh-Amid[13] controlled the initial microstructure of CK60 steel to decrease the spheroidization time isothermally held at 973 K (700 °C). They reported that unstable initial microstructure, such as that in the case of martensite, required much less time to transform into the spheroidized microstructure. Yi *et al.*[14] added aluminum to 0.78 pctC-1.49 pctMn eutectoid steel to accelerate spheroidization. The addition of aluminum as a ferrite former increased the A_{e3} temperature, which resulted in the refinement of interlamellar spacing during cooling and increased the A_{c1} temperature, which induced a higher spheroidization temperature causing higher carbon diffusivity.

Induction heating is a non-contact heating process used to generate heat in a metal sample by employing eddy currents. The sample can be heated to a very high temperature that is sufficient for the material to begin melting in a few seconds. Recently, several researchers have reported that induction heat treatment is more effective than conventional heat treatment in reducing the tempering process time. Nam *et al.*[15,16] investigated the relationship between microstructure features and mechanical properties of steels tempered by induction heat treatment. Their work mainly characterized the effects of adding Cr and Mo as well as tempering temperature on mechanical properties. The maximum tempering temperature used in their study was 973 K (700 °C), with an isothermal holding time limited to 40 seconds. Lee *et al.*[17] compared induction heat treatment to conventional heat treatment for tempering of steels with a focus on the dependence of carbide precipitation with the addition of carbide formers such as Cr and Mo. They reported that the tempering time for carbide spheroidization was reduced by induction heating when a tempering temperature of 993 K (720 °C) and a holding time of only 15 seconds are used. Xie *et al.*[18] investigated the microstructure and precipitation behavior of a microalloyed steel sample tempered by high-frequency induction treatment with a tempering temperature of 873 K (600 °C) and holding time of 15 minutes. They found that this process resulted in the formation of nanoscale carbides during induction tempering. Revilla *et al.*[19] investigated the effect of heating rate on the microstructure and carbide formation during induction tempering of a low-alloy steel tempered at 973 K (700 °C) for 1260 seconds and found that the carbide particle size became smaller as a result of increased heating rate and decreased holding time.

Although induction tempering has been rather extensively studied in the last several years, little attention has been given to the induction spheroidization of steels. In the present study, therefore, the spheroidization of the medium-carbon 1045 steel was investigated by comparing the induction treatment method with conventional heat treatment method. The relationship between cementite formation and mechanical properties was evaluated with the aim of improving the mechanical properties and reducing the spheroidization time.

II. EXPERIMENTAL PROCEDURE

The chemical composition of 1045 steel used in this study is listed in Table I. A bar with a diameter of 20 mm was hot rolled after reheating to 1473 K (1200 °C) to make a 2 mm-thick sheet sample. Tensile test specimens were machined from the hot-rolled sheet parallel to the rolling direction according to the ASTM E8 standard. The tensile specimens were then austenitized at 1123 K (850 °C) for 30 minutes in a tube furnace under vacuum (to prevent surface oxidation) and immediately quenched in water, resulting in a fully martensitic microstructure. Conventional spheroidization treatment was performed by quenching specimens and then heat treating them at 973 K (700 °C) in a vacuum furnace to a maximum isothermal holding time of 24 hours. The specimens were then furnace cooled to room temperature. The induction spheroidization treatment was completed by quenching specimens and heating them to 973 K (700 °C) at a heating rate of about 63 K s^{-1} for a maximum holding time of 15 minutes followed by air cooling. The mechanical properties of heat-treated specimens were evaluated by tensile tests and microhardness measurements at room temperature. A strain rate of 1×10^{-3} s^{-1} was used in the tensile testing. An optical microscope (OM) and field-effect emitter scanning electron microscope (FE-SEM) were used to observe the microstructures of quenched and spheroidized specimens as well as the fracture surface of specimens after tensile testing. The volume fraction and size of cementite particles were observed by FE-SEM. Energy dispersive spectroscopy (EDS) analysis with a scanning electron microscope (SEM) was performed to analyze carbides in the spheroidized specimens.

III. RESULTS AND DISCUSSION

Figure 1 shows the optical and SEM micrographs of the quenched 1045 specimen before spheroidization. The fully martensitic microstructure was only observed

Table I. Chemical Composition of 1045 Steel (in Weight Percent)

C	Si	Mn	P	S	Cu	Ni	Cr	Mo	Al	Fe
0.47	0.2	0.69	0.018	0.012	0.14	0.06	0.12	0.01	0.01	bal.

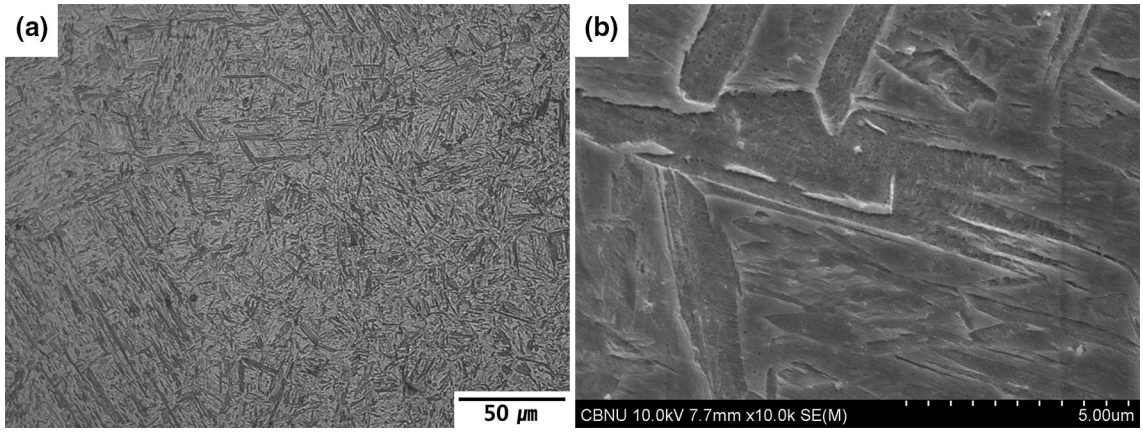

Fig. 1—(*a*) Optical micrograph and (*b*) SEM micrograph of the as-quenched 1045 specimen.

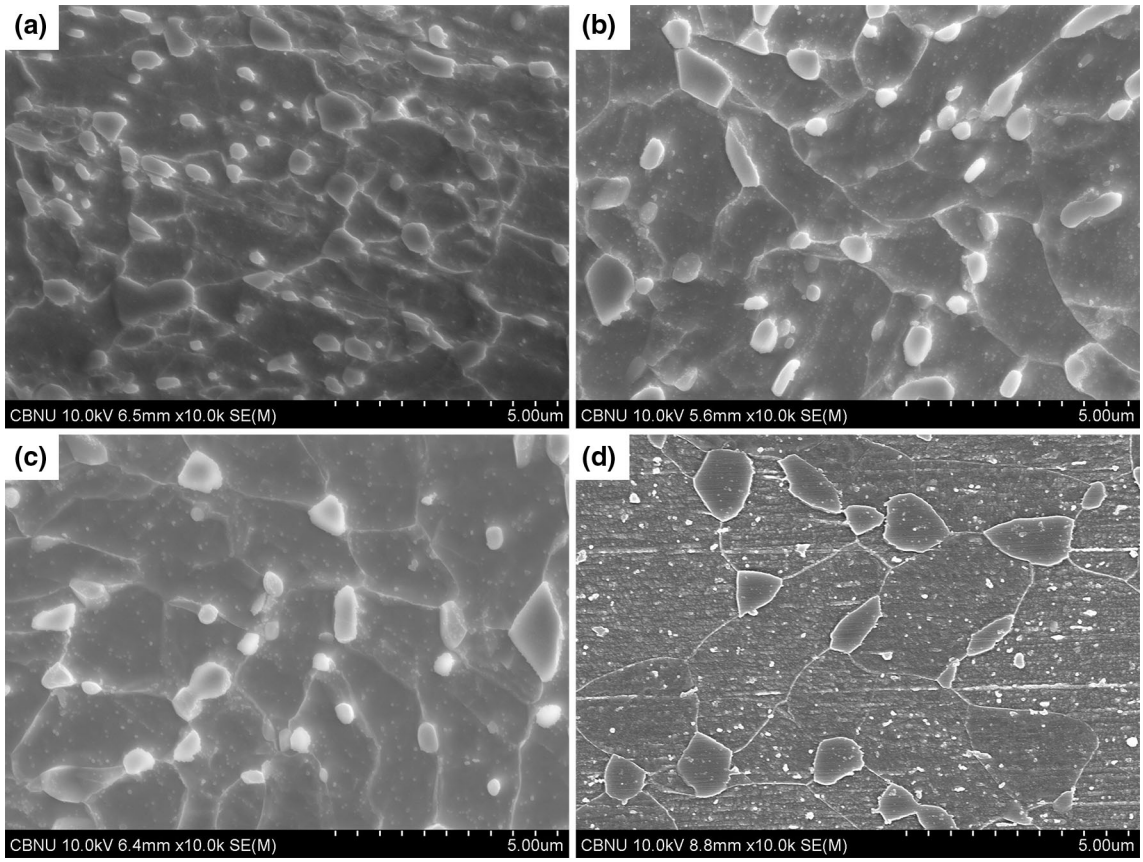

Fig. 2—SEM micrographs of the spheroidized specimens in the tube furnace at 973 K (700 °C) for different holding times: (*a*) 180 min, (*b*) 360 min, (*c*) 720 min, and (*d*) 1440 min.

because direct quenching into water was sufficiently fast to minimize any diffusional transformation above the martensite start temperature.

Figure 2 shows SEM micrographs of the spheroidized specimens in the tube furnace at 973 K (700 °C). It is evident that average particle size increases with holding

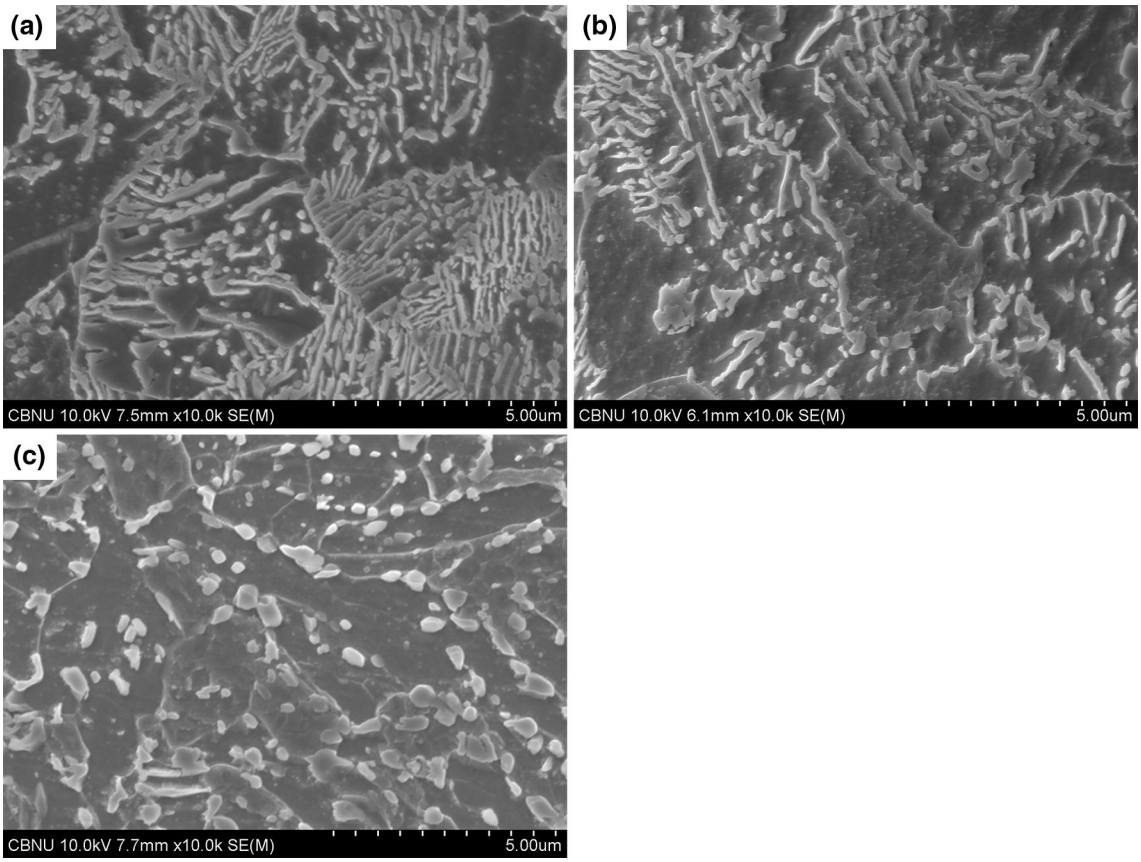

Fig. 3—SEM micrographs of the spheroidized specimens by the induction heating at 973 K (700 °C) for different holding times: (*a*) 5 min, (*b*) 10 min, and (*c*) 15 min.

time. Very coarse particles of approximately 2 μm were observed in the specimen held for 1440 minutes as shown in Figure 2(d). The spherical particles are cementite (Fe_3C).

The thermodynamic calculations for the chemical composition (Table I) were performed using JMatPro 8.0 software (Sente Software Ltd., Surrey, UK) with the database of General Steels, to evaluate the volume fraction of all possible phases. The stable phases at 973 K (700 °C) were austenite, ferrite, and MnS, whose volume fractions were 0.93081, 0.06886, and 0.00033, respectively. It has been predicted that the other carbide phases, *e.g.*, M_7C_3, could be precipitated below 673 K (400 °C) and that the Cu precipitate is stable below 823 K (550 °C). The calculated A_{e1} temperature at which the austenite appeared during heating was 986 K (713 °C). The actual A_{c1} temperature is higher than the equilibrium temperature A_{e1} depending on the heating rate. Thus, no austenite could be formed during the spheroidization at 973 K (700 °C), regardless of the heating rate.

Figure 3 shows the SEM micrographs of the spheroidized specimens that underwent the induction heat treatment at 973 K (700 °C). An abundance of rod-type cementite particles with a small amount of spherical cementite particles were observed when the specimen was held for 5 minutes as shown in Figure 3(a). As the holding time increased, the rod-shaped cementite particles gradually broke into smaller spherical particles (Figure 3(b)) and only the spheroidized cementite particles were subsequently distributed all over the ferrite matrix (Figure 3(c)). These spherical particles grew in size with time at elevated temperature. Interestingly, it was noted that the spherical cementite particles in Figure 3(a) had been formed from broken rod-shaped cementite, which is very similar to the spheroidization of the pearlite microstructure.[20] The production of the rod-shaped particles occurs at the beginning of spheroidization by the induction heat treatment. Before heating, the carbon atoms were supersaturated in quenched martensite. Due to the fast induction heating to 973 K (700 °C), small cementite particles were able to precipitate in all possible nucleation sites at once. If the cementite particles precipitated along grain boundaries, they could merge and subsequently form rod-shaped cementite particles. Otherwise, spherical particles could be formed initially in a matrix and grown. Lee *et al.*[17] also observed the large carbide agglomerates along the grain boundary in 0.45C steel tempered at 723 K (450 °C) by high-frequency induction heat treatment.

Figure 4 compares the relative volume fractions of cementite that varies with spheroidization conditions. The relative volume fraction of cementite was calculated by dividing the measured volume fraction of cementite by the equilibrium volume fraction of cementite. The equilibrium volume fraction of cementite at 973 K

(700 °C) was found to be 0.069 by JMatPro calculation. About 92 vol pct of cementite was observed in the specimen spheroidized in the tube furnace and held for 180 minutes. All cementite was precipitated in the case of the 1440-minute holding time. For the induction heat treatment, approximately 83 vol pct of cementite was formed after a 5-minute holding time, regardless of the cementite particle shape, and over 90 vol pct of cementite precipitated after holding for 15 minutes. These results indicate that the rate of cementite formation when the induction heat treatment was used was higher than that when the conventional vacuum furnace heat treatment was used. The induction heat treatment could produce a given volume fraction of carbide particles in a shorter period of time, which is about one-tenth the time that was required by the furnace heat treatment.

Figure 5 shows the variation of the average spheroidized cementite particle size with respect to spheroidization time: The average size increased gradually with holding time, irrespective of the heat treatment method. The specimen held for 1440 minutes in the furnace exhibited the maximum size of spheroidized cementite particles, *i.e.*, >550 nm. Typically, the diffusion-controlled particle growth at a temperature can be expressed in terms of an Arrhenius-type equation as follows. An assumption is that the particle shape remains spherical.

$$d = A \exp\left(-\frac{Q}{RT}\right) t^n, \qquad [1]$$

where d is the diameter of particle, Q is the activation energy for growth, R is the gas constant, T is an isothermal temperature, t is a holding time, A is constant, and n is a time exponent. Equation [1] can be simplified as the temperature is fixed, given by

$$d = k\, t^n, \qquad [2]$$

where k is the temperature-independent constant. Based on the experimental data as indicated in Figure 5, an empirical equation to predict the average size of spherical cementite particles in 1045 steel which is isothermally held at 973 K (700 °C) is derived in Eq. [3] as a function of the holding time.

$$d = 121.78\, t^{0.214}, \qquad [3]$$

where d is the diameter of cementite particle in μm and t is the spheroidizing time in min. All experimental data points lie on the same curve regardless of the method of heating. On the other hand, the growth rate of the cementite particle (in Figure 5) shows very high at the beginning of spheroidization, which decreases significantly until about 100 minutes of spheroidization time and then gradually slows down as the spheroidization is progressed. This indicates that an adequate volume fraction of spheroidized cementite particles with controlled particle size can be achieved by induction in a short heating time.

Figure 6 compares the engineering stress–strain curves for the tensile specimens heat treated under different conditions. The maximum tensile strength and total elongation of the as-quenched specimen were 908 MPa and 0.49 pct, respectively. This as-quenched specimen was very brittle due to its fully developed martensitic microstructure and fractured without plastic deformation. After the specimens were spheroidized in the furnace, the ductility was improved as shown in Figure 6(a). A maximum elongation of 30 pct was observed for the specimen held for 720 minutes. The tensile strength was incrementally decreased from 549 to 450 MPa with the holding time. Both strength and elongation decreased in the specimen spheroidized for 1440 minutes, as a result of coarsening of particles that were over 550 nm in size. This indicates that increasing the volume fraction of cementite particles and suppressing the particle coarsening simultaneously are important to achieving a balance between strength and ductility. Compared with the furnace heat treatment, the specimens spheroidized by the induction heat treatment exhibited higher strength and lower ductility, as shown in Figure 6(b). The tensile strength of these specimens decreased from 724 to 681 MPa with increasing holding

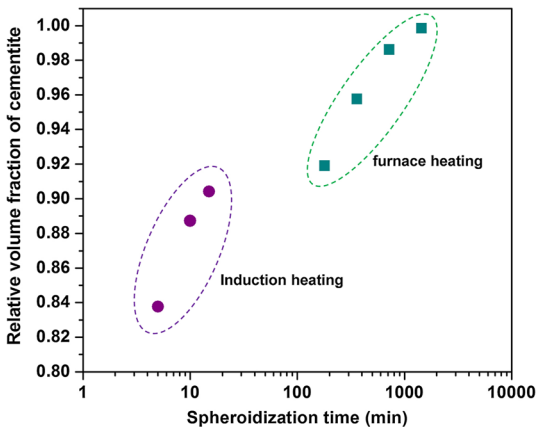

Fig. 4—The relative volume fraction of cementite varied with different spheroidization conditions.

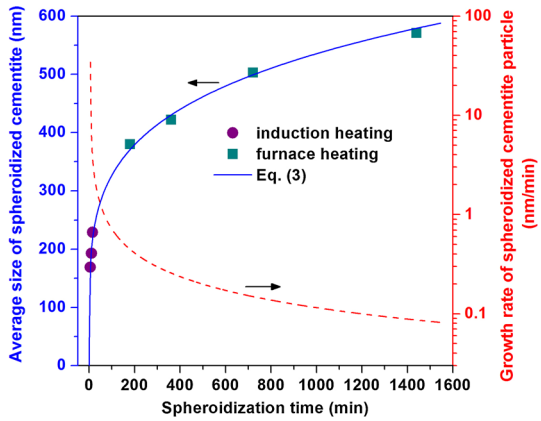

Fig. 5—Variations of the average size of spheroidized cementite particle calculated using Eq. [3] (blue solid line) and the growth rate of spheroidized cementite particles (red dash line) according to the spheroidization time. The symbols represent the experimental data obtained by different heating methods (Color figure online).

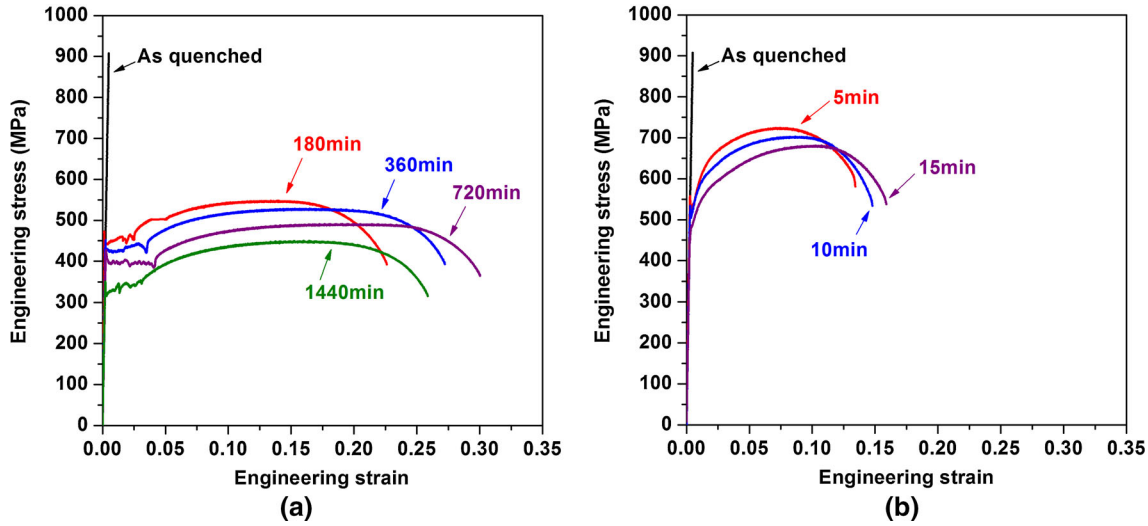

Fig. 6—Engineering stress–strain curves of 1045 steel spheroidized with different heat treatment conditions: (*a*) furnace heat treatment and (*b*) induction heat treatment. The time indicates the spheroidizing time at 973 K (700 °C).

time, whereas elongation increased from 13.4 to 15.9 pct, thus showing that the induction heat treatment effectively improves the ductility of 1045 steel.

Yield point elongation was observed after furnace spheroidization. Similar yield point elongations of spheroidized steels have been observed in other studies.[21–23] However, no obvious yield point elongation was observed after the induction heat treatment. The yield point elongation is mainly observed in low-carbon steels, due to the interaction between the solute C or N (even in a few ppm) and dislocations.[24] By the thermodynamic calculation, the equilibrium carbon solubility in α-ferrite at 973 K (700 °C) was 86 ppm for 1045 steel with the chemical composition in Table I. When the specimen was held at 973 K (700 °C) for a long time sufficient to diffuse carbon atoms into the octahedral sites of α-ferrite, some solute carbon atoms may have remained in solution. Then, the remained solute carbon atoms could affect the yield point elongation, as observed in Figure 6(a).

Figure 7 shows the variation in mechanical properties with varying cementite volume fraction. Increasing the volume fraction of cementite resulted in a decrease in the yield stress, tensile stress, and hardness, while the elongation increased, resulting in softening of steel. Both the yield stress and hardness linearly decreased with the volume fraction of cementite regardless of heating methods. The two-step variation of tensile stress and elongation could be affected not only by the volume fraction of cementite but also by the average size of spheroidized cementite particles. The average size of spheroidized cementite is obviously increased with spheroidization time as the heating method is changed, as shown in Figure 5. This confirms that the volume fraction of cementite directly affects the mechanical properties of spheroidized steels. However, the strength and ductility could deteriorate due to the coarsening of particles.

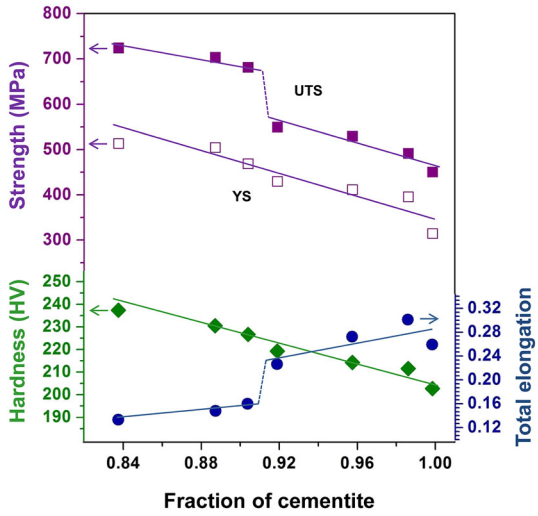

Fig. 7—Mechanical properties varied with the volume fraction of cementite in the spheroidized specimens.

We investigated the effect of combining the two different heat treatments for improving the elongation within a short spheroidization time. In addition, the induction heat treatment and the furnace heat treatment were sequentially applied. A specimen was heated up to 973 K (700 °C) and held for 15 minutes by induction heating and then immediately moved into the furnace where the temperature was maintained at the same holding temperature of 973 K (700 °C). Continuously, the specimen was heat treated in the furnace for 180 minutes and furnace cooled to room temperature. The tensile test and the microstructural analysis were performed under the same condition, as explained in Section II. Figure 8 shows the experimental results for the specimen spheroidized sequentially by the induction

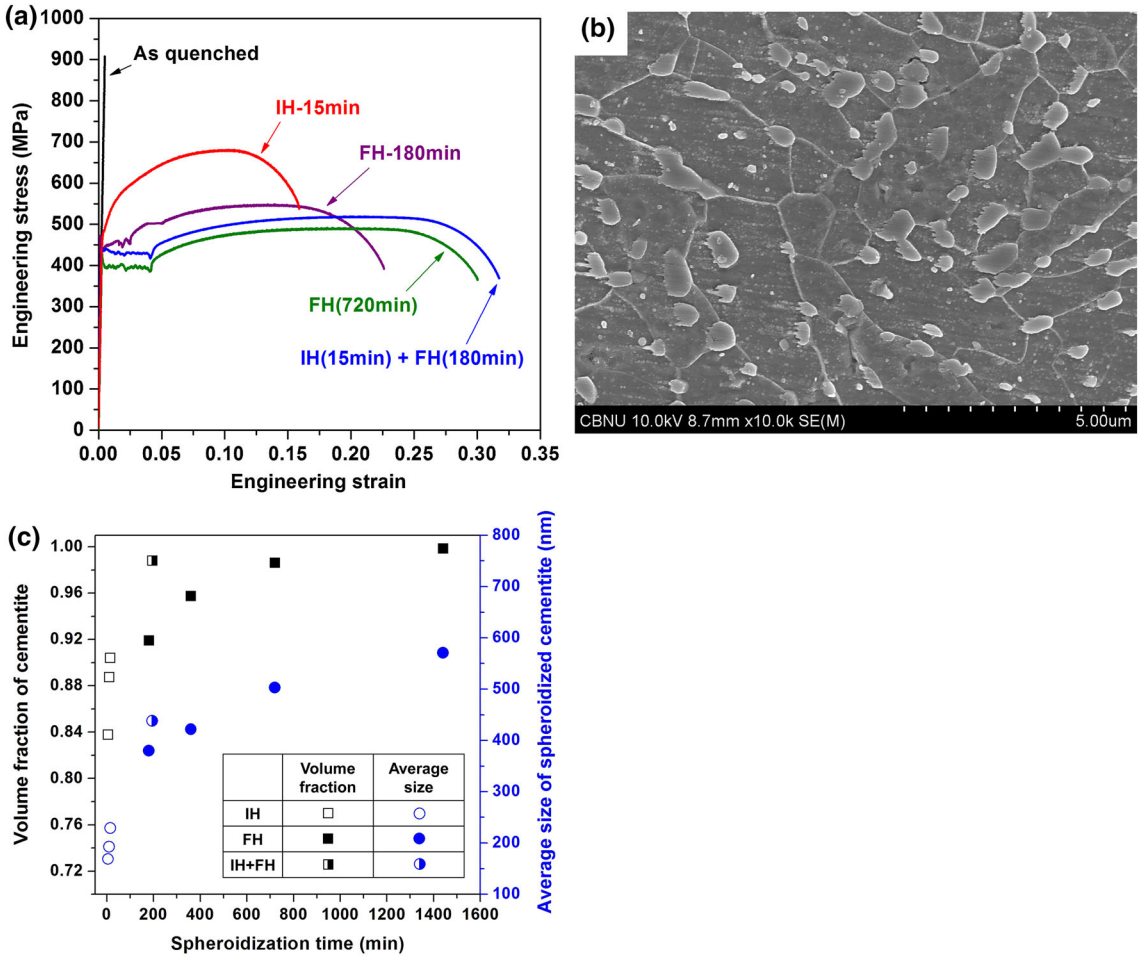

Fig. 8—(*a*) Stress–strain curve, (*b*) SEM micrograph, and (*c*) characteristics of cementite particles of the specimen spheroidized sequentially by the induction heat treatment (IH) and furnace heat treatment (FH). The spheroidizing times are indicated for each stress–strain curve.

heat treatment and furnace heat treatment. The elongation and the tensile stress of the combined spheroidized specimen were 31.7 pct and 517 MPa, respectively. These properties are superior to those of the specimen spheroidized in the furnace for 720 minutes; this indicates the superior microstructure of the specimen spheroidized sequentially. The average size of spheroidized cementite particles of the specimen subjected to both heat treatments was about 438 nm, which was slightly larger than the average particle size of 422 nm in the specimen spheroidized in the furnace for 360 minutes. Furthermore, the relative volume fraction of cementite was 98.8 vol pct in the specimen subjected to both heat treatments. To obtain this volume fraction by furnace heat treatment alone would require a holding time in excess of 720 minutes. The SEM micrograph of the combined spheroidized specimen is shown in Figure 8(b) and the characteristics of the cementite particles are compared in Figure 8(c).

Figure 9 compares the fracture surface of the tensile specimens prepared by different heat treatments. The as-quenched specimen was very brittle and predominately displayed intergranular fracture, whereas the spheroidized specimens showed typical ductile fracture with dimpled morphology. The size of dimples increased with the total holding time regardless of heating methods. These dimples develop as voids are formed from secondary particles such as cementite or inclusions.[25] Secondary particles were observed in dimples. Figure 10 shows the SEM image of a dimple fracture surface from a tensile specimen spheroidized in the tube furnace for 1440 minutes. It was confirmed that the particle in the dimple was cementite. Therefore, the relationship between the increase in the size of dimples and the average size of spheroidized cementite particles could be identified by comparing Figures 9(b) through (d) with Figure 8(c); it is clear that the size of dimples increased proportionally with the size of secondary particles.

IV. CONCLUSIONS

In the present work, the effects of induction heat treatment on the microstructure and mechanical properties of spheroidized AIS 1045 steel have been investigated. The volume fraction and size of spherical cementite particles in the sample spheroidized by the

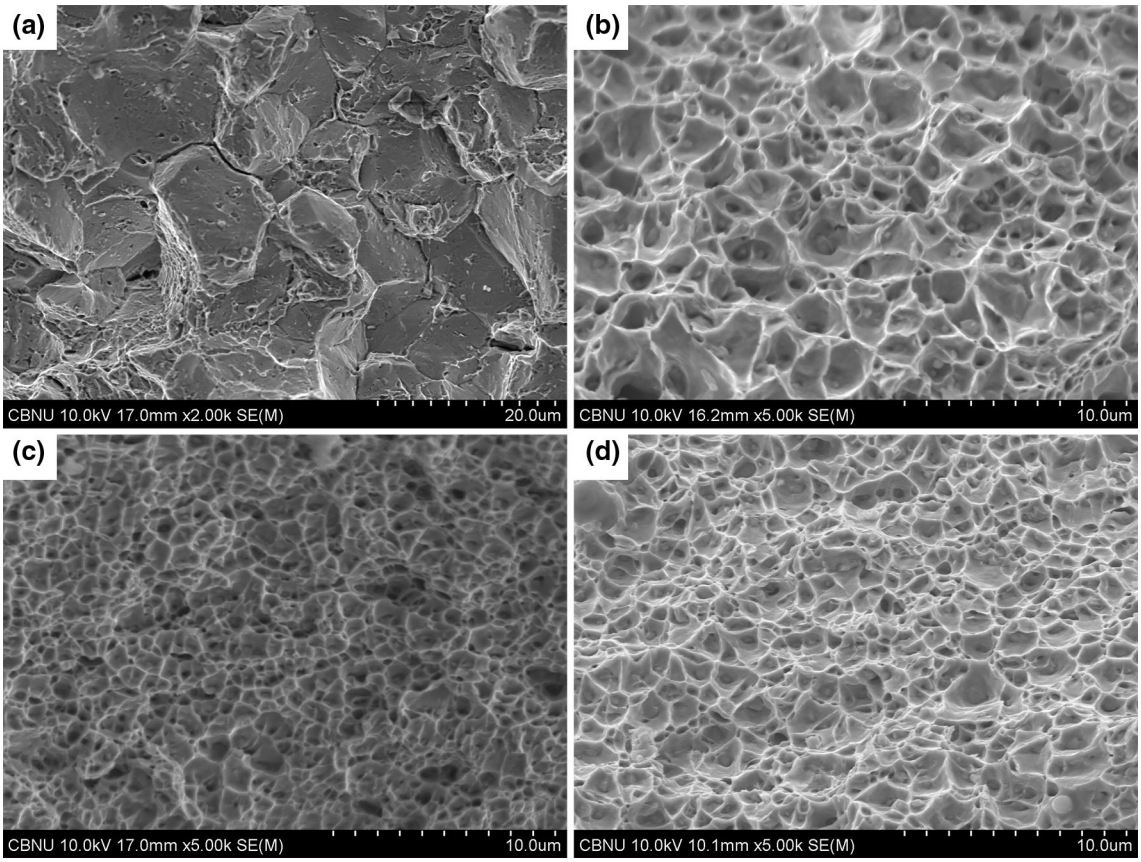

Fig. 9—SEM images of fracture surface from the tensile specimens with various heat treatment conditions: (*a*) as-quenched, (*b*) furnace heat treated for 1440 min, (*c*) induction heat treated for 15 min, and (*d*) induction heat treated for 15 min followed by furnace heat treated for 180 min.

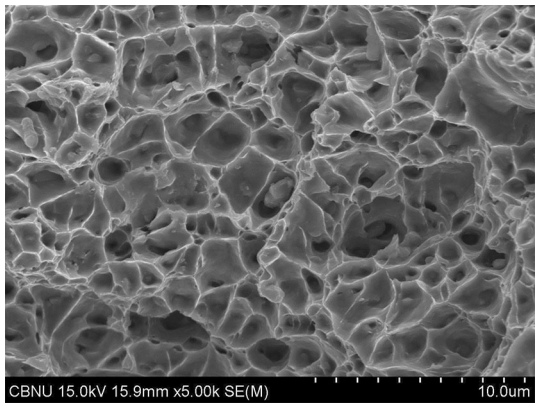

Fig. 10—SEM image of fracture surface from the tensile specimen spheroidized in the tube furnace for 1440 min.

induction treatment are compared to those in samples prepared by the furnace heat treatment. The obtained results were as follows:

1. The volume fraction of cementite particles controls the tensile properties regardless of heat treatment methods, resulting in a decrease in the yield stress, tensile stress, and hardness and an increase in elongation with increasing volume fraction of cementite. The decrease in elongation was due to coarsening for particles that were over 550 nm in size.
2. Compared to furnace heating, induction heating can achieve greater volume fraction of cementite particles prior to the onset of excessive particle coarsening. This results in higher elongation for any particular strength in a short heating time.
3. The combination of the induction spheroidization and furnace spheroidization results in superior mechanical properties and a reduction in the total heat treatment time due to the high volume fraction of spherical cementite particles and the suppression of particle coarsening.

ACKNOWLEDGMENT

MK and SJL gratefully acknowledge the support by Business for Academic-industrial Cooperative establishments funded by the Korea Small and Medium

Business Administration in 2014 (Grant No. 1503002010).

REFERENCES

1. G. Krauss: *Steels-Processing, Structure, and Performance*, ASM International, Materials Park, OH, 2005, pp. 251–62.
2. L. Ratke and P.W. Voorhees: *Growth and Coarsening—Ostwald Ripening in Material Processing*, Springer, New York, NY, 2002, pp. 117–66.
3. C.C. Chou, P.W. Kao, and G.H. Cheng: *J. Mater. Sci.*, 1986, vol. 21, pp. 3339–44.
4. A. Saha, D. Kumar Mondal, and J. Maity: *Mater. Sci. Eng. A*, 2010, vol. 527, pp. 4001–07.
5. A. Saha, D. Kumar Mondal, and J. Maity: *J. Mater. Eng. Perform.*, 2011, vol. 20, pp. 114–19.
6. Z.Q. Lv, B. Wang, Z.H. Wang, S.H. Sun, and W.T. Fu: *Mater. Sci. Eng. A*, 2013, vol. 574, pp. 143–48.
7. S.E. Nam and D.N. Lee: *J. Mater. Sci.*, 1987, vol. 22, pp. 2319–26.
8. S.L. Zhang, X.J. Sun, and H. Dong: *Mater. Sci. Eng., A*, 2006, vol. 432, pp. 324–32.
9. W.Y. Guo, J. Li, and X.F. Jiang: *J. Mater. Eng. Perform.*, 2012, vol. 21, pp. 1003–07.
10. J. Arruabarrena, B. López, and J.M. Rodriguez-Ibabe: *Metall. Mater. Trans. A*, 2014, vol. 45A, pp. 1470–84.
11. J.M. O'Brien and W.F. Hosford: *J. Mater. Eng. Perform.*, 1997, vol. 6, pp. 69–72.
12. H.J. Li, B.Q. Wang, X.Y. Song, S.Z. Guo, and N.J. Gu: *J. Iron Steel Res. Int.*, 2006, vol. 13, pp. 9–13.
13. A. Karnyabi-Gol and M. Sheikh-Amid: *J. Iron Steel Res. Inter.*, 2010, vol. 17, pp. 45–52.
14. H.L. Yi, Z.Y. Hou, Y.B. Xu, D. Wu, and G.D. Wang: *Scr. Mater.*, 2012, vol. 67, pp. 645–48.
15. W.J. Nam, D.S. Kim, and S.T. Ahn: *J. Mater. Sci.*, 2003, vol. 38, pp. 3611–17.
16. S.T. Ahn, D.S. Kim, and W.J. Nam: *J. Mater. Proc. Tech.*, 2005, vol. 160, pp. 54–58.
17. J.B. Lee, N. Kang, J.T. Park, S.T. Ahn, Y.D. Park, I.D. Choi, K.R. Kim, and K.M. Cho: *Mater. Chem. Phys.*, 2011, vol. 129, pp. 365–70.
18. Z.J. Xie, Y.P. Fang, G. Han, H. Guo, R.D.K. Misra, and C.J. Shang: *Mater. Sci. Eng. A*, 2014, vol. 618, pp. 112–17.
19. C. Revilla, B. Lopez, and J.M. Rodriguez-Ibabe: *Mater. Design*, 2014, vol. 62, pp. 296–304.
20. O.E. Atasoy and S. Ozbilen: *J. Mater. Sci.*, 1989, vol. 24, pp. 281–87.
21. Z.L. Zhang, Y.N. Liu, J.W. Zhu, and G. Yu: *Mater. Sci. Eng. A*, 2008, vols. 483–484, pp. 64–66.
22. Y. Xiong, T. He, Z. Guo, H. He, F. Ren, and A.A. Volinsky: *Mater. Sci. Eng. A*, 2013, vol. 563, pp. 163–67.
23. Y.W. Lee, Y.I. Son, and S.J. Lee: *Mater. Sci. Eng. A*, 2013, vol. 585, pp. 94–99.
24. B. Soenen, A.K. De, S. Vandeputte, and B.C. De Cooman: *Acta Mater.*, 2004, vol. 52, pp. 3483–92.
25. Samsul. Rizal and Hirromi. Homma: *Int. J. Impact Eng.*, 2000, vol. 24, pp. 69–83.